*Proc. Natl. Acad. Sci. USA*
Vol. 82, pp. 4404–4408, July 1985
Cell Biology

# Theoretical problems related to the attachment of microtubules to kinetochores

**(two-phase kinetic model/GTP cap/capture of centrosomal microtubule)**

TERRELL L. HILL

Laboratory of Molecular Biology, National Institute of Arthritis, Diabetes, and Digestive and Kidney Diseases, National Institutes of Health, Bethesda, MD 20205

*Contributed by Terrell L. Hill, January 30, 1985*

**ABSTRACT** **A possible model is analyzed for the maintenance of attachment of a shortening microtubule (MT) to a kinetochore. In this model it is assumed that a MT is inserted and held in a sleeve or channel of the outer layer of a kinetochore while subunits are lost from the MT tip through the central layer of the kinetochore. A second problem considered is the elementary bioenergetics of MT growth and shortening, as associated with the presence or absence of a GTP cap on the MT ends. The free-energy source is the hydrolysis of GTP in solution. The third problem discussed is the kinetics of capture of a centrosomal MT by a target (e.g., a kinetochore).**

The two-phase macroscopic kinetic model (1) of the end of a microtubule (MT) is used as the basis for the discussion below. The two phases refer to possible gross states of a MT end, which can either have a GTP cap (2) or not have such a cap. A MT end with a GTP cap is stable; an end without a cap is unstable (3). The two-phase kinetic model arose from a series of theoretical and experimental studies (1–7). Various consequences have been examined elsewhere (8–12).

It is somewhat puzzling how pole-to-kinetochore MTs in anaphase can shorten (lose subunits) while remaining attached to a kinetochore. A simple quantitative model is presented here that might provide a possible mechanism; it is based on an idea introduced in figure 23*B* of ref. 13. Actually, it is not certain that shortening occurs at the kinetochore end of pole-to-kinetochore MTs. However, for concreteness, this assumption is made here. In any case, the analysis shows in principle how a "sleeve" can provide a stable attachment for a shortening MT end.

Another related topic considered is the simple bioenergetic basis of MT growth from a centrosome, capture of the free MT end by a target (e.g., a kinetochore) followed by shortening of the MT from the target end, which has the effect of pulling the target in to the centrosome.

The third topic examined is the mean time required for a target to capture a centrosomal MT, at steady state.

## Model for Microtubule Shortening

Part of a three-layered kinetochore is shown schematically in Fig. 1. The outer layer is assumed to furnish channels or sleeves for MT insertion. The MT is shown schematically as a two-stranded structure. The attachment of a MT is due to attractive forces between the MT subunits and the wall of the sleeve. It is assumed that subunits can be lost (or gained) from the end of the inserted MT via the inner unoccupied part of the sleeve and the central layer of the kinetochore (which, in photographs, appears much less dense than the other layers).

If the outer layer is, say, 400 Å thick (14), then the sleeve could accommodate (when full) about $M = 65$ subunits (tubulin dimers). The thickness and $M$ may be larger than this. We keep track of the position of the MT end in a sleeve by the integer $n = 1, 2, \ldots, M$. Fig. 1*a* shows a MT end at an arbitrary value of $n$; Fig. 1*b* shows the two extremes, $n = 1$ (fully inserted) and $n = M$ (almost unattached).

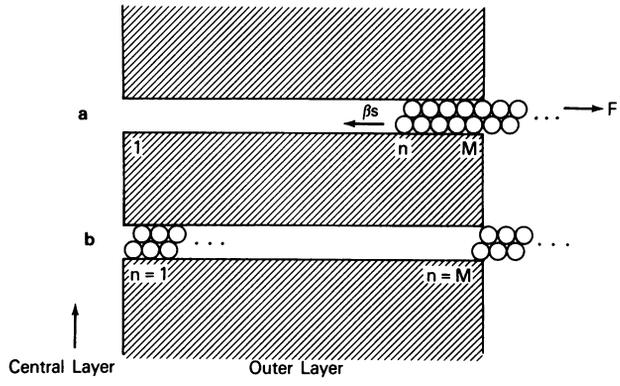


FIG. 1. Schematic picture of a MT (shown as two-stranded) held by a sleeve or channel in the outer layer of a kinetochore. (*a*) Arbitrary position $n$ of the MT tip. (*b*) Extreme positions of the MT tip ($n = 1$, $M$) in the sleeve.

Our object is to calculate the steady-state distribution in $n$—i.e., to see where the MT end is likely to locate itself inside a sleeve. We now consider in turn the several physical features that are involved in this problem; these contribute the various factors that appear in the rate constants (Fig. 2*a*) that govern the random walk of the MT end on the integers $n = 1, \ldots, M$. The steady-state distribution in $n$, calculated numerically, then follows directly from Fig. 2*a*.

The steps in the random walk ($\Delta n = \pm 1$) are of length $l = 6.15$ Å. The diffusion coefficient of a chromosome is $D = kT/\zeta = \kappa l^2$, where $\zeta$ is the friction coefficient and $\kappa$ is the rate constant for discrete steps of length $l$, corresponding to $D$. From $F_{ch} = \zeta v$, where $F_{ch} = 10^{-8}$ dyne (1 dyne = 10 $\mu$N) is the resisting force of a chromosome moving toward the pole with velocity $v = 1\ \mu\text{m}\cdot\text{min}^{-1}$ (15), we find $\zeta = 6 \times 10^{-3}$ g·sec$^{-1}$ and then $\kappa \cong 1800\ \text{s}^{-1}$.

Let $w$ be the (negative) free energy of interaction of a subunit in a MT with the wall of a sleeve. For a MT at $n$, this free energy is $(M - n)w$. This effect tends to pull the MT into the sleeve ($n \rightarrow 1$); see figure 23*B* of ref. 13. A step to the right in Fig. 1*a* or 2*a* increases the free energy of the MT by $-w$. Hence, $\kappa$ in Fig. 2*a* for steps to the right must be modified to $\kappa s$, where $s \equiv e^{w/kT} < 1$.

A significant $w$ (see below) implies close contact between MT and sleeve. As a consequence of molecular "roughness," one might expect a resistance or potential barrier to movement of the MT in the sleeve that increases linearly with the depth of the MT. This is indicated schematically in Fig. 2*b*,

The publication costs of this article were defrayed in part by page charge payment. This article must therefore be hereby marked "*advertisement*" in accordance with 18 U.S.C. §1734 solely to indicate this fact.

Abbreviation: MT, microtubule.

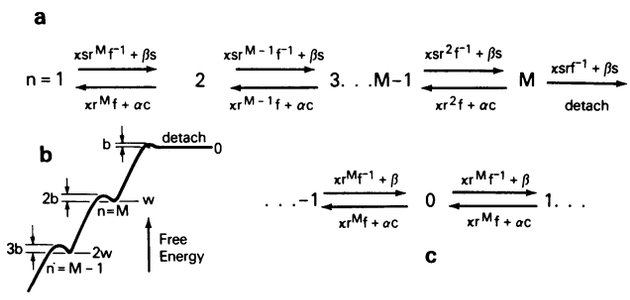


FIG. 2. (*a*) Kinetic diagram and rate constants for a random walk of the MT tip when inserted in a sleeve. (*b*) Schematic free-energy curve showing the origin of parameters $s = e^{w/kT}$ and $r = e^{-b/kT}$. (*c*) Extension of scheme in *a* to $n < 1$, which is necessary if there is significant population at $n = 1$ (the MT penetrates into the central layer).

where the unit potential barrier is $b$. We define $r \equiv e^{-b/kT} < 1$. The factors $r, r^2, \ldots, r^M$ included in Fig. 2*a* take care of this effect. These factors would have no influence on an *equilibrium* distribution of $n$ (they cancel if $\beta s$ and $\alpha c$ are omitted from Fig. 2*a*) but they do have the effect, in the steady state of interest here (with $\beta s$ and $\alpha c$ included), of limiting the extent of penetration of the sleeve by the MT because the steps at small $n$ become relatively slow.

Because of the frictional resistance of the chromosome to movement, there is an effective (positive) force $F$ (Fig. 1*a*) tending to pull the MT out of the sleeve (13). Because there may be 30 or 40 MTs attached to a kinetochore, $F$ might be of order $F_{ch}/35 = 10^{-8}/35$ dyne. The thermodynamic effect of $F$ is that the free energy of the MT decreases by an amount $Fl$ if $n \rightarrow n + 1$. We assume that this free energy is split equally between forward and backward rate constants, so that a factor $f^{-1}$ appears in the rate constant for $n \rightarrow n + 1$ in Fig. 2*a* and a factor $f$ appears in $n + 1 \rightarrow n$, where $f \equiv e^{-Fl/2kT} < 1$. Thus $F$ favors larger values of $n$ (less penetration). Actually, with the value of $F$ mentioned above, $f = 0.99979$; hence this effect is negligible. If $F$ is 100 times larger, $f = 0.979$. Even in this case the effect of $F$ is quite small.

So far we have discussed the motion of an intact MT in the sleeve. The value of $n$ can also change by gain or loss of individual subunits from the tip of the MT (see the arrow labeled $\beta s$ in Fig. 1*a*). The $\alpha$ end of a MT is the end attached to a kinetochore. This end is in the unstable shortening phase (no cap); see the Introduction. The rate constant $\beta$ here is the same as $-J_{2\alpha}$ at $c = 0$ in ref. 7 or ref. 12; that is, $\beta = 340\ s^{-1}$. We approximate $J_{2\alpha}(c)$ (figure 3 of ref. 12) by $\alpha c - \beta$ here, where $c$ is the local subunit concentration (in the central layer and sleeves) and $\alpha$ is the small average slope of $J_{2\alpha}(c)$. When a single subunit is added to or lost from a MT in a sleeve, an extra free energy $w$ (interaction of the subunit with the wall of the sleeve) is involved. We assume that this affects $\beta$ but not $\alpha$ (diffusion controlled). Hence $\beta$ is reduced to $\beta s$ in the sleeve (it is harder for a subunit to break loose). The rate constants $\beta s$ and $\alpha c$ are included in Fig. 2*a*. Loss of subunits from the MT tip tends to increase the $n$ values of the steady-state distribution.

For simplicity in the calculations below, we now assume that $\alpha c$ is small and can be neglected in Fig. 2*a* (primarily because $\alpha$ is small). The rate of loss of subunits from an attached MT is then $\beta s$. The rate of movement of a chromosome toward the pole is about 1 $\mu m \cdot min^{-1}$ (15), which corresponds to the loss of about 27 subunits $s^{-1}$ from the attached MTs. Hence we take $\beta s = 27\ s^{-1}$ and $s = 27/340$. This value of $s$ corresponds to $w \cong -1500$ cal·mol$^{-1}$ (1 cal = 4.18 J).

Fig. 3 shows illustrative steady-state probability distributions $p_n$ calculated numerically from Fig. 2*a* using $\kappa = 1800\ s^{-1}$, $s = 27/340$, $M = 65$, $f = 1$, $\alpha c = 0$, and $\beta = 340\ s^{-1}$. All of these distributions are quite satisfactory. That is, the MT can lose subunits at 27 $s^{-1}$ but still remain attached indefinitely. The peak in the $n$ distribution (see below) moves to $n = 48.1$ at $r = 0.8$ and to $n = 55.0$ at $r = 0.7$. In the latter case there would be a small rate of MT detachment from position $n = M$ (Fig. 2*a*). Hence we require, for indefinite MT stability in the sleeve in this example, $r > 0.7$.

If $r = 0.93$, the peak in $n$ is at 9.8; there will be a small probability $p_1$ at $n = 1$. Hence for $r \geq 0.93$, the kinetic scheme has to be extended as in Fig. 2*c* into the region $n < 1$ (the MT penetrates into the central layer). However, there are only very limited possibilities in this range of $r$ because it is generally not possible to keep the rate of subunit loss as low as 27 $s^{-1}$ (note $\beta$, not $\beta s$, in Fig. 2*c*), even by reducing $s$ (when $s = 0$, the largest possible $r$, with rate of subunit loss 27 $s^{-1}$, is 0.9386). Hence the practical range in $r$, with the other parameters chosen in this illustration, is $0.7 < r < 0.9386$.

The maximum in the steady-state $n$ distribution, used above, can be calculated as follows. Let $n_{max}$ be the required location of the maximum in $p_n$ and let $n^*$ be the value of $n$ that gives equal forward and backward rate constants between $n^*$ and $n^* + 1$ (Fig. 2*a*):

$$\kappa s r^{M-n^*+1} f^{-1} + \beta s = \kappa r^{M-n^*+1} f + \alpha c. \qquad [1]$$

If we solve this equation for $n^*$, then $n_{max} = n^* + 1/2$. Thus we find

$$n_{max} = M + \frac{3}{2} - \frac{\ln R}{\ln r}, \qquad [2]$$

where

$$R \equiv \frac{\beta s - \alpha c}{\kappa(f - sf^{-1})}.$$

**Simplified Bioenergetics of the Two-Phase Model**

An idealized and simple treatment of the basic bioenergetics of growing (capped) and shortening (uncapped) MTs is presented here. Despite the simplicity, this analysis is adequate to understand the essentials of the problem. The qualitative background for this discussion is given in ref. 11 and the quantitative background is in ref. 13 (section IV A).

In the equations, we use T to refer to GTP·tubulin and D to refer to GDP·tubulin. The chemical potentials of these two species, as monomers at concentrations $c_T$ and $c_D$, are

$$\mu_T = \mu_T^0 + RT \ln c_T \qquad [3]$$

$$\mu_D = \mu_D^0 + RT \ln c_D. \qquad [4]$$

Similar expressions apply for $\mu_{GTP}$, $\mu_{GDP}$, and $\mu_P$, the chemical potentials in solution of GTP, GDP, and $P_i$. The

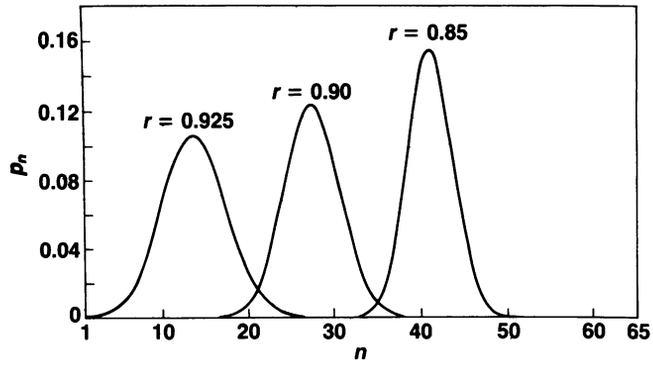


FIG. 3. Examples of the steady-state distribution $p_n$ (probability of the MT tip being at position $n$). In all three cases the MT tip is losing subunits at the rate 27 $s^{-1}$ but the MT is stable in the sleeve.

concentrations of all of the above five species are considered as steady-state constants, below.

If GTP·tubulin monomer aggregates to form GTP·tubulin polymer (i.e., a hypothetical MT in which GTP hydrolysis is inhibited), the chemical potential of the GTP·tubulin polymer, denoted by $\mu_{\square T}$, is independent of $c_T$. Let $c_T^e$ be the (critical) concentration of GTP·tubulin monomer at which GTP·tubulin monomer and GTP·tubulin polymer are in equilibrium. Then, at equilibrium,

$$\mu_{\square T} = \mu_T^0 + RT \ln c_T^e. \quad [5]$$

If we use this relation in Eq. 3 to eliminate $\mu_T^0$,

$$\mu_T(c_T) = \mu_{\square T} + RT \ln (c_T/c_T^e). \quad [6]$$

An analogous equation applies to GDP·tubulin monomer and polymer (see below). Fig. 4 includes $\mu_{\square T}/RT$ (constant) and $\mu_T/RT$ as a function of $\ln(c_T/c_T^e)$. If GTP·tubulin polymerizes at a concentration $c_T > c_T^e$ (in the example in Fig. 4, $c_T = e^5 c_T^e = 148.4 c_T^e$), the process is spontaneous and the free-energy change per mol (negative) is

$$\Delta\mu_1 = \mu_{\square T} - \mu_T(c_T) = -RT \ln (c_T/c_T^e). \quad [7]$$

The quantity $\Delta\mu_1$ is shown in Fig. 4.

With GTP·tubulin polymer formed, we imagine the inhibition on GTP hydrolysis to be lifted so that GTP·tubulin polymer transforms spontaneously into GDP·tubulin polymer (i.e., a MT with GDP·tubulin subunits), with release of $P_i$ into the solution. The constant chemical potential of GDP·tubulin polymer is denoted $\mu_{\bigcirc D}$. The free-energy change per mol (negative) for this process is (Fig. 4)

$$\Delta\mu_2 = (\mu_{\bigcirc D} + \mu_P) - \mu_{\square T}. \quad [8]$$

The symbols □ and ○ are used in $\mu_{\square T}$ and $\mu_{\bigcirc D}$ to indicate a likely conformational change in tubulin (11), as a consequence of the hydrolysis of GTP. The fact that $\Delta\mu_2$ is negative is a consequence of the hydrolysis of GTP on the polymer. Also included in $\Delta\mu_2$ is the positive free-energy change associated with the change in two-dimensional crystal structure, GTP·tubulin polymer → GDP·tubulin polymer.

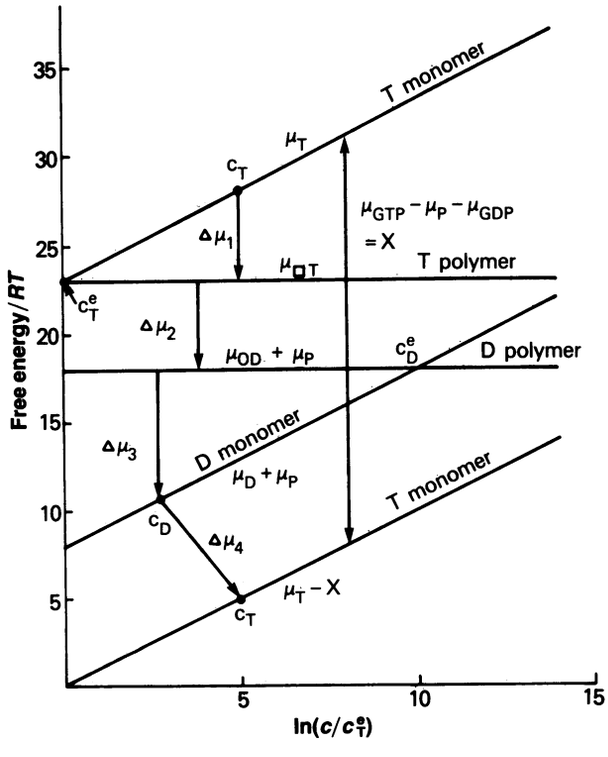


FIG. 4. Illustrative free-energy levels, as functions of free subunit concentrations, for the cycle in Eq. 11.

The relative instability of the GDP·tubulin polymer is reflected in a much larger critical concentration $c_D^e$ (Fig. 4) for formation of GDP·tubulin polymer from GDP·tubulin monomer, compared with $c_T^e$ for the formation of GTP·tubulin polymer from GTP·tubulin monomer (in the example in Fig. 4, $c_D^e/c_T^e = e^{10} = 2.2 \times 10^4$). As a consequence, at a typical concentration $c_D < c_D^e$, GDP·tubulin polymer will disassemble from the ends into GDP·tubulin monomer at concentration $c_D$. In Fig. 4, $c_D = c_T/10$ is used, which is realistic (16). The spontaneous process GDP·tubulin polymer → GDP·tubulin monomer at $c_D$ has a free-energy change (Fig. 4) per mol (negative) of

$$\Delta\mu_3 = \mu_D(c_D) - \mu_{\bigcirc D} = RT \ln (c_D/c_D^e). \quad [9]$$

The final process ($\Delta\mu_4$) included in Fig. 4 is the spontaneous exchange of GTP for GDP on GDP·tubulin monomer at $c_D$ to produce GTP·tubulin monomer at $c_T$. The free-energy change per mol (negative) is

$$\Delta\mu_4 = (\mu_T + \mu_{GDP}) - (\mu_D + \mu_{GTP}). \quad [10]$$

The four processes above (Eqs. 7–10) comprise a cycle:

$$\text{GTP·tubulin monomer} \xrightarrow{1} \text{GTP·tubulin polymer} \xrightarrow{2} \text{GDP·tubulin polymer} \xrightarrow{3} \text{GDP·tubulin monomer} \xrightarrow{4} \text{GTP·tubulin monomer}. \quad [11]$$

In this cycle the tubulin returns unchanged to its initial state (GTP·tubulin monomer at $c_T$) but the cycle does have the net consequence that 1 mol of GTP in solution has been hydrolyzed to GDP + $P_i$ in solution for each mol of tubulin converted into polymer. The total free-energy change (negative) for the cycle, per mol of tubulin, is

$$\Delta\mu_1 + \Delta\mu_2 + \Delta\mu_3 + \Delta\mu_4 = -X, \quad [12]$$

$$X \equiv \mu_{GTP} - \mu_{GDP} - \mu_P. \quad [13]$$

$X$, a positive quantity, is the thermodynamic force (17) that drives the cycle, Eq. 11. It is the force $X$ that makes it possible, in Fig. 4, to have both GTP·tubulin polymer more stable than GTP·tubulin monomer and GDP·tubulin monomer more stable than GDP·tubulin polymer.

As shown in Fig. 4, the initial free-energy level of the system is $\mu_T(c_T)$ whereas the final free-energy level is $\mu_T(c_T) - X$. The value of $X/RT$ chosen in Fig. 4 is 23.0, which corresponds to $X = 13.6$ kcal·mol$^{-1}$ (1 cal = 4.18 J) at 25°C.

We turn now to the more realistic case of MTs growing from centrosome sites until possible capture by a target, e.g., a kinetochore. We use the same idealized model as above. Starting with an empty centrosome nucleated site, the initial section of polymer formed on the site is GTP·tubulin polymer. The free-energy change per mol is $\Delta\mu_1$ (Eq. 7). After the lag period between aggregation and hydrolysis (2), all further polymer growth in effect adds GTP·tubulin to the free tip of the MT and simultaneously converts GTP·tubulin to GDP·tubulin (by hydrolysis) at the base of the GTP cap, the cap having been created by the "initial section of polymer" mentioned above. Thus, as this second and principal stage of growth proceeds, the cap maintains a constant size at the tip of the MT and the net process is GTP·tubulin monomer →

GDP·tubulin polymer. That is, the growth appears as lengthening GDP·tubulin polymer, which extends from the centrosome site to the base of the GTP·tubulin cap. The associated free-energy change per mol in this second stage of growth is $\Delta\mu_1 + \Delta\mu_2$.

If the tip of the MT loses its cap by a fluctuation (free-energy change per mol of cap, $\Delta\mu_2$) before the tip is captured, the MT will then shorten from the tip back to the empty centrosome site (free-energy change per mol, $\Delta\mu_3 + \Delta\mu_4$). In this case an amount of free energy $X$ per mol of polymer formed has been expended to pay for the exploratory mission by the MT tip (11).

If, however, the MT tip is captured by, say, a kinetochore, with cessation of growth, the GTP cap will be lost by hydrolysis (free-energy change per mol, $\Delta\mu_2$). The MT will then shorten (free-energy change per mol, $\Delta\mu_3 + \Delta\mu_4$), pulling the target to the centrosome. Again an amount of free energy $X$, per mol of polymer formed, will have been expended. However, in this case, if the target offers a steady resisting force $F$ to the attached polymer as it shortens, some of $\Delta\mu_3$ (and $X$) is converted into mechanical work (see p. 54 of ref. 13). The amount of this work, per subunit of polymer formed, is $Fl$, where $l$ = 6.15 Å. The overall efficiency of free-energy conversion, $Fl/X$ ($X$ here is per molecule of GTP, not per mol), is generally very small (13). The main value of the GTP free-energy expenditure in MTs (11) would appear to be to make possible both growth and rapid shortening, as in the Eq. **11** cycle.

### Mean Time Required for a Target to Capture a Microtubule

We begin this section by considering the relatively simple capture of a centrosomal MT by an isolated nearby target. The second topic discussed is the more complicated capture of a centrosomal MT by a kinetochore (target) in the metaphase plate of chromosomes.

Suppose that a centrosome with $N$ nucleated sites has a *steady-state* distribution of MTs emanating from these sites, in the presence of a free subunit concentration $c$. The MTs are assumed to project outward from the centrosome in a completely random way (with spherical symmetry). Suppose further that there is an isolated small target for capture of a MT at a distance $d$ from the centrosome. The target has a capture cross-sectional area $A$ normal to the line between target and centrosome. What is the mean time $\bar{t}$ for capture of a MT by the target?

A MT that can just reach the target has $\nu = d/l$ subunits, where $l$ = 6.15 Å. The steady-state probability that any one nucleated site of the centrosome has on it a growing MT with $m$ subunits is $P_m(c)$, where $P_m$ is given by equation 35 of ref. 8. The mean steady-state current (number per unit time) of MT tips crossing the entire spherical surface of radius $d$ about the centrosome, in the outward (growing) direction, is $NP_\nu(c)J_1(c)$, where $J_1(c)$ is the mean rate of growth (subunits·s$^{-1}$) of the $\alpha$ (or +) end of a MT when this end is capped (i.e., the end is in phase 1). The probability that any MT tip crossing this spherical surface will hit the target is $A/4\pi d^2$ (because $A << 4\pi d^2$). Hence $\lambda$, the mean number of hits per unit time, is given by

$$\lambda = NP_\nu(c)J_1(c)(A/4\pi d^2). \quad [14]$$

The mean time between hits, or the mean lifetime of a new target before it captures a MT, is $\bar{t} = 1/\lambda$. A numerical example is given below.

If $c$ is very close to $c_\alpha$ (the critical concentration for the $\alpha$ end), most steady-state MTs will be much larger than any reasonable value for $\nu = d/l$, and hence $P_\nu$ will be extremely small. Also, if $c$ is very small, very few steady-state MTs will be as large as $\nu$ so that $P_\nu$ will again be extremely small. For any specified $\nu$, $P_\nu(c)$ will have a maximum at a $c$ in the neighborhood of that $c$ which makes $\bar{m} = \nu$, where $\bar{m}$ is the mean steady-state MT size (equation 44 of ref. 8).

We turn now to a numerical example. For rate constants of the two-phase kinetic model (1, 8), including $c$ dependence, we use equations 2, 3, and 6 of ref. 12 (for the $\alpha$ end). In this case, the critical concentration for the $\alpha$ end is $c_\alpha$ = 9.75 $\mu$M. During mitosis, $c$ will be reduced below $c_\alpha$ by the extensive MT polymerization (11). Values of $10^5P_\nu$, from equation 35 of ref. 8, for $c$ = 6, 7, and 8 $\mu$M and for $d$ = 5, 7.5, and 10 $\mu$m (for which $\nu$ = 8130, 12,195, and 16,260, respectively) are given in Table 1.

We complete the calculation of $\lambda$ and $\bar{t}$ (Eq. **14**) for the particular case $c$ = 6 $\mu$M, $d$ = 5 $\mu$m (Table 1). We assume $N$ = 250 (mitotic centrosome) and take $A$ as the area ($\pi a^2$) of a circle of radius $a$ = 0.25 $\mu$m (used below for a kinetochore). Then $A/4\pi d^2 = 6.25 \times 10^{-4}$. At the above $c$, $J_1$ = 31.73 s$^{-1}$. Using $P_\nu$ from Table 1, Eq. **14** then gives $\lambda = 2.01 \times 10^{-4}$ s$^{-1}$ and $\bar{t}$ = 82.7 min, a very long time. This is a consequence of the very small target and the very small value of $P_\nu$ (the steady-state $P_m$ is spread out over a very wide range in $m$; $P_m = P_0x^m$, $x$ = 0.999879).

**Capture of a MT by a Kinetochore.** We idealize by assuming that the metaphase plate of chromosomes completely fills the plane of a circle of radius $b$. The center of this circle is a distance $d$ from the centrosome (pole) of interest, along a line normal to the plane of the circle. A circular kinetochore (target), of radius $a$, is located at the center of the large circle ($b >> a$). How long does it take this target to capture a centrosomal MT at steady state? We sketch the solution below. However, not enough information is available to permit a definitive numerical calculation.

The essential new feature here is that a significant number of MTs growing out from the centrosome hit the metaphase plate. Such a MT will stop adding new subunits (ref. 13, pp. 71–75), which normally replenish the GTP cap; hence, the cap will deteriorate by hydrolysis. This will be followed by shortening of the MT (i.e., phase 1 → phase 2) and detachment from the plate. However, while the MT tip is on the metaphase plate (i.e., while the cap is deteriorating), the tip may diffuse in two dimensions to the small target (kinetochore) and be captured. Thus, the plate acts as a relatively large interim collecting device for the ultimate small target (18).

For simplicity, we treat all MTs that hit the metaphase plate as having a length $d$ and $\nu = d/l$ subunits (it is tedious but not difficult to avoid this simplification). The kinetic diagram for any one of these MTs is shown in Fig. 5. Thus the usual diagram (figure 6, ref. 8) for an uninhibited centrosomal MT is cut off and turned around at $m = \nu$. The new rate constant $k_o$ is the reciprocal of the mean time it takes for the GTP cap of a MT that has reached the metaphase plate to deteriorate sufficiently by hydrolysis to allow MT shortening to begin (phase 2). The mean hydrolysis rate constant $\kappa$ for GTPs in a cap is 0.25 min$^{-1}$ (2). In the time $1/\kappa$, 63% of the GTPs in a cap will have been hydrolyzed. Hence, as a reasonable guess, we take $k_o$ = 0.25 min$^{-1}$ = 4.167 × 10$^{-3}$ s$^{-1}$, independent of $c$. Because $k_o << J_1$, $P^*_\nu$ will be quite large (the asterisk refers to the truncated diagram in Fig. 5). Considered as a random walk problem, there is delayed reflection at $m = \nu$ in Fig. 5.

Table 1. Values of $10^5P_\nu$ in an example

| | $d$, $\mu$m | | |
|---|---|---|---|
| $c$, $\mu$M | 5 | 7.5 | 10 |
| 6 | 4.06 | 2.48 | 1.52 |
| 7 | 3.38 | 2.59 | 1.99 |
| 8 | 2.21 | 1.93 | 1.68 |

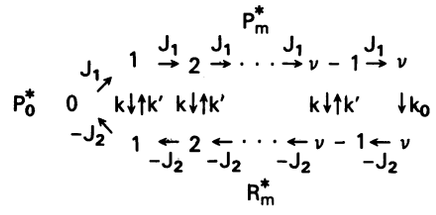


FIG. 5. Kinetic diagram for a centrosomal MT that encounters the metaphase plate of chromosomes at $m = \nu$. The upper states (probabilities $P^*_m$) are in phase 1 (GTP cap); the lower states are in phase 2 (no GTP cap), with probabilities $R^*_m$. $J_2$ is negative.

The steady-state probability distribution in Fig. 5 is easy to find:

$$P^*_\nu = (J_1P^*_0/k_o)x^{\nu-1},\ P^*_m = P^*_0\, x^m \quad (m = 1, \ldots, \nu - 1) \qquad [15]$$

$$R^*_m = (J_1P^*_0/-J_2)x^{m-1} \quad (m = 1, \ldots, \nu) \qquad [16]$$

$$P^*_0 = \frac{-k_0J_2(1 - x)}{k_0(J_1 - J_2) - J_1J_2x^{\nu-1} - (k_0J_1 - k_0J_2 - J_1J_2)\,x^\nu} \qquad [17]$$

$$x \equiv J_1(k' - J_2)/ - J_2\,(k + J_1). \qquad [18]$$

The subscript $\alpha$ (for the $\alpha$ end) has been dropped from these rate constants. Note that $J_2$ is negative.

For the same numerical example as in Table 1 (plus the $k_o$ value above), $P^*_\nu$ and $10^5P^*_{\nu-1}$ have been calculated and are given in Tables 2 and 3. Note that $P^*_{\nu-1}$ is larger than $P_\nu$ (because of the reflection at $m = \nu$) and that $P^*_\nu$ is much larger than both of these (by a factor of $\approx 10^4$). MTs that hit the plate spend a significant fraction ($P^*_\nu$) of their steady-state lifetimes in contact with the plate.

The mean number ($\lambda^*$) of *direct* hits of the kinetochore per unit time by growing MTs will be given by Eq. **14** but with $P^*_{\nu-1}(c)$ in place of $P_\nu(c)$. Tables 1 and 3 show that $\lambda^* > \lambda$ (Eq. **14**), but $\lambda^*$ is still small. The direct hits will, however, be supplemented by a presumably much larger number of *indirect* hits ($\delta^*$ per unit time) from MT tips on the metaphase plate.

We adopt the model of Adam and Delbrück (18) to find an expression for $\delta^*$. Let $N^*$ be the number of centrosomal MTs (out of $N = 250$) that grow in the direction of the plate. (From a consideration of the solid angle involved, $N^*$ may be of order 20.) Hence the mean number of MT tips on the plate at steady state is $N^*P^*_\nu$. Let $\tau$ be the mean time required for any one of these tips to diffuse in the circle (plate) of radius $b$ to the small target of radius $a$. Because $b >> a$, a good approximation to $\tau$ is (18)

$$\tau \cong (b^2/2D)[\ln(b/a) - 0.50], \qquad [19]$$

Table 2. Values of $P^*_\nu$ in an example

| | $d$, $\mu$m | | |
|---|---|---|---|
| $c$, $\mu$M | 5 | 7.5 | 10 |
| 6 | 0.331 | 0.197 | 0.119 |
| 7 | 0.422 | 0.295 | 0.212 |
| 8 | 0.484 | 0.368 | 0.288 |

Table 3. Values of $10^5P^*_{\nu-1}$ in an example

| | $d$, $\mu$m | | |
|---|---|---|---|
| $c$, $\mu$M | 5 | 7.5 | 10 |
| 6 | 4.34 | 2.59 | 1.56 |
| 7 | 4.74 | 3.32 | 2.39 |
| 8 | 4.75 | 3.61 | 2.83 |

where $D$ is the two-dimensional diffusion coefficient of a MT tip on the plate. Then the number of indirect hits of the target per unit time is $\delta^* = N^*P^*_\nu/\tau$. Finally, the mean lifetime of a kinetochore (target) before a hit of either kind is

$$\bar{t}^* = 1/(\lambda^* + \delta^*), \qquad [20]$$

which is presumably much smaller than $\bar{t}$ above.

We can estimate $a$ as $\approx 0.25$ $\mu$m and $b$ as $\approx 3$ $\mu$m if $d = 5$ $\mu$m ($N^*/N$ and $b/d$ must be self-consistent), but $D$ is unknown. The difficulty is that $D$ is determined by the brownian motion of the entire MT, which is anchored at the centrosome, but this motion is restrained at the tip by the molecular roughness on the plate and by the fact that the MT is pushing against the plate (ref. 13, pp. 71–75). The resistance to the motion of the MT tip on the plate is difficult to judge. An experimental estimate of $\bar{t}^*$ would allow a calculation of $D$, using Eq. **20**.

To illustrate the calculation of $D$ in this way, suppose that lines drawn from the two ends of a diameter of the metaphase plate to the centrosome form an angle of 60° at the centrosome. Then

$$N^*/N = (2 - \sqrt{3})/4 = 0.0670,$$
$$N^* = 16.7,\ b = d/\sqrt{3}. \qquad [21]$$

Using $a = 0.25$ $\mu$m, $d = 5$ $\mu$m, and $c = 6$ $\mu$M, we find from Tables 2 and 3 and Eq. **20** that if $\bar{t}^* = 2$, 4, or 6 min, then we require $D = 11.9$, 5.8, and $3.8 \times 10^{-11}$ cm$^2$·s$^{-1}$, respectively. These values happen to be in the range found for protein molecules diffusing laterally in a membrane.

I thank Marc Kirschner, Tim Mitchison, and Bruce Nicklas for stimulating comments.

1. Hill, T. L. & Chen, Y. (1984) *Proc. Natl. Acad. Sci. USA* **81**, 5772–5776.
2. Carlier, M.-F. & Pantaloni, D. (1981) *Biochemistry* **20**, 1918–1924.
3. Carlier, M.-F., Hill, T. L. & Chen, Y. (1984) *Proc. Natl. Acad. Sci. USA* **81**, 771–775.
4. Hill, T. L. & Carlier, M.-F. (1983) *Proc. Natl. Acad. Sci. USA* **80**, 7234–7238.
5. Chen, Y. & Hill, T. L. (1983) *Proc. Natl. Acad. Sci. USA* **80**, 7520–7523.
6. Mitchison, T. & Kirschner, M. W. (1984) *Nature (London)* **312**, 232–237.
7. Mitchison, T. & Kirschner, M. W. (1984) *Nature (London)* **312**, 237–242.
8. Hill, T. L. (1984) *Proc. Natl. Acad. Sci. USA* **81**, 6728–6732.
9. Hill, T. L. (1985) *Proc. Natl. Acad. Sci. USA* **82**, 431–435.
10. Chen, Y. & Hill, T. L. (1985) *Proc. Natl. Acad. Sci. USA* **82**, 1131–1135.
11. Mitchison, T. & Kirschner, M. W. (1984) in *Molecular Biology of the Cytoskeleton*, eds. Borisy, G. G., Cleveland, D. W. & Murphy, D. B. (Cold Spring Harbor Laboratory, Cold Spring Harbor, NY), pp. 27–44.
12. Chen, Y. & Hill, T. L. (1985) *Proc. Natl. Acad. Sci. USA*, in press.
13. Hill, T. L. & Kirschner, M. W. (1982) *Int. Rev. Cytol.* **78**, 1–125.
14. DeRobertis, E. D. P. & DeRobertis, E. M. F. (1980) *Cell and Molecular Biology* (Saunders, Philadelphia), 7th Ed., p. 391.
15. Nicklas, R. B. (1965) *J. Cell Biol.* **25**, 119–135.
16. Neidl, C. & Engel, J. (1979) *Eur. J. Biochem.* **101**, 163–169.
17. Hill, T. L. (1977) *Free Energy Transduction in Biology* (Academic, New York).
18. Adam, G. & Delbrück, M. (1968) in *Structural Chemistry and Molecular Biology*, eds. Rich, A. & Davidson, N. (Freeman, San Francisco), pp. 198–215.